

18B.2 EXTRATROPICAL CONVECTIVE PRECURSORS TO INITIATION OF MJO CONVECTION OVER THE INDIAN OCEAN

Jennifer A. Gahtan* and Paul E. Roundy
University at Albany-State University of New York, Albany, New York

1. INTRODUCTION

As the most prominent mode of intraseasonal variability over the tropics, the Madden-Julian Oscillation (MJO) consists of alternating periods of deep enhanced and suppressed convection coupled to planetary scale circulation that propagates eastward with a globally averaged speed of around 5 m/s (Zhang 2005).

Though MJO deep convection often organizes over the western Indian Ocean and strengthens over the Indian and western Pacific Ocean warm pool, anomalous cloud activity associated with the MJO is prevalent over many other regions including extratropical eastern Africa, and Southeast Asia (Barlow and Wheeler 2005, Oetli et al. 2014). In particular, convection over these regions is typical prior to the formation of Indian Ocean deep convection. Though previous work has attributed this extratropical convection to increased moisture advection from lower-level anticyclones forced by an equatorial Rossby wave response to MJO suppressed convection over the Indian Ocean, a thorough analysis of these precursors may provide insight on MJO convective initiation.

2. DATA

The National Oceanic and Atmospheric Administration (NOAA) outgoing longwave radiation (OLR) data are used as a proxy for convection (Liebmann and Smith 1996). OLR data are on a 2.5-degree grid daily from 1975-2012 and units are in watts per square meter. Anomalies from climatology are calculated by subtracting the annual cycle and its first three harmonics. To isolate the intraseasonal signal, OLR data are Lanczos filtered for 20-100 days using 201 weights (Duchon 1979). ECMWF Reanalysis-Interim wind data from 1988-2009 are used (Dee et al. 2011).

3. TIME-EXTENDED LATITUDINAL EOF INDEX

To achieve better insight about potential tropical-extratropical intraseasonal interaction over Africa, Southeast Asia, and the Indian Ocean, an index centered on the region is created through the use of time-extended latitudinal Empirical Orthogonal Function

(EOF) analysis. Physically, this index represents the most prevalent spatial-temporal patterns of the 20-100 day OLR in a latitude-lag diagram averaged over 20-70E and will hereafter be called the intraseasonal meridional mode index (IMMI).

The OLR data is first centered on the smoothed climatological latitudinal minima in OLR. The 20-70E averaged latitude-time sequence of 20-100 day OLR is calculated for 40 degrees south of to 40 degrees north of each OLR minima for 25 days before to 25 days after every day over the entire time series. Two-dimensional EOFs are calculated for the resulting dataset. The leading two EOFs are rotated by their median phase difference from the widely used Real-time Multivariate MJO (RMM) index (Wheeler and Hendon 2004) to obtain maximal correspondence. This rotation does not create new signal in the index, but simplifies comparison with commonly used indices.

20-100 day OLR Averaged 20-70E

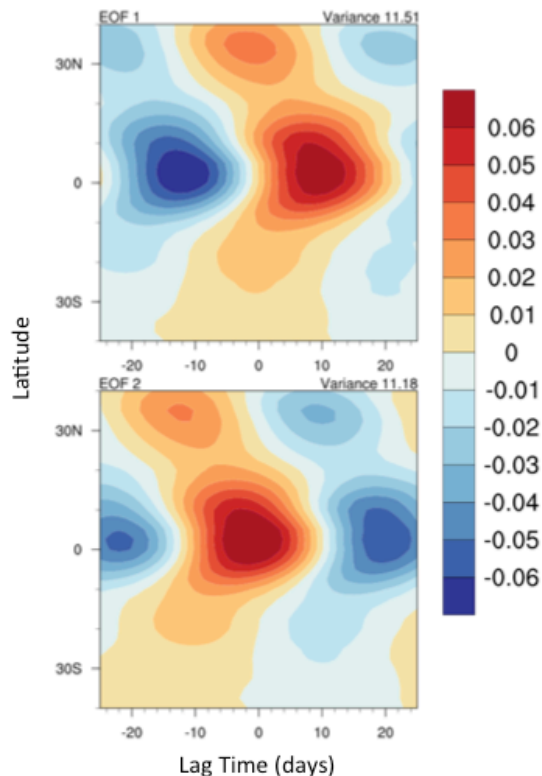


Figure 1: The leading two time-extended latitudinal EOFs of the 20-100 day OLR averaged over 20-70E.

* Corresponding author address: Jennifer A. Gahtan, SUNY Albany, Dept. of Atmos. and Env. Sci., Albany, NY; email: jgahtan@albany.edu

Phase 1 OLR Anomaly Averaged 15S-15N

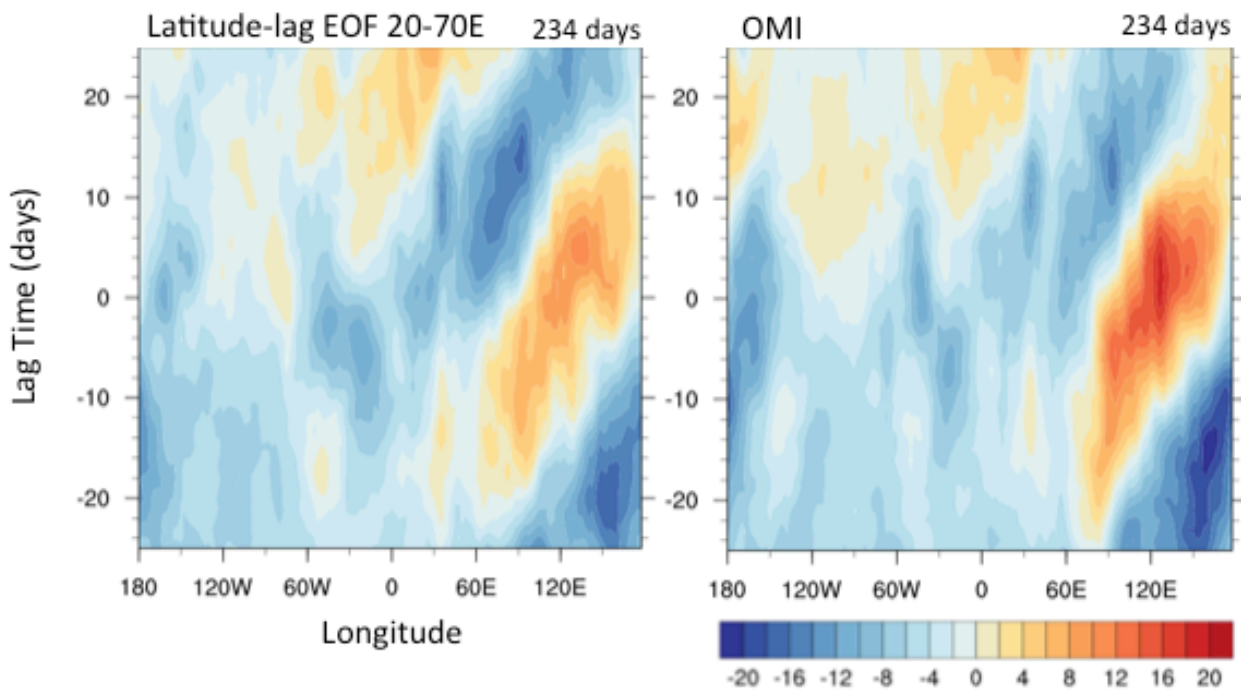


Figure 2: Time longitude diagram of OLR anomalies centered on phase 1 for IMMI and OMI.

Figure 1 shows the leading two EOFs after rotation. The variance accounted for by the first two EOFs is 11.51% and 11.18%, respectively. EOF1 shows an equatorial center of anomalous convection from days -25 through -5. Starting around day -15, suppressed convective anomalies begin to form over the extratropics of both hemispheres. In the Northern Hemisphere the signal is centered about 32 degrees north of the ITCZ; the southern hemispheric signal does not have a center, but strengthens as the signal moves northwards and forwards in time. These extratropical signals trace farther equatorward with time, becoming continuous with the equatorial MJO convection. Both equatorial and extratropical signals last around 20 days. The equatorial signals have a meridional scale of about 30 degrees latitude. EOF2 has a similar structure to and is in quadrature with EOF1, with the signal shifted approximately 11 days earlier relative to lag 0.

4. COMPOSITE ANALYSIS

Signals in various fields associated with the leading PCs are identified through the use of composites created in a manner similar to Wheeler and Hendon 2004. Composites are centered on phase 1, when MJO convection starts organizing over the western Indian Ocean and are calculated for days when the amplitude of the index is greater than one during December through February. The OLR MJO Index (OMI, Kiladis et al. 2014) is used for comparison.

Figure 2 shows the time versus longitudinal structure of OLR anomalies averaged over 15N-15S for IMMI and OMI centered on lag zero for phase 1. Though the chosen region of 20-70E is not one typically associated with strong MJO deep convection, IMMI

OLR Anomaly and 200hPa Wind Avg. 20-70E

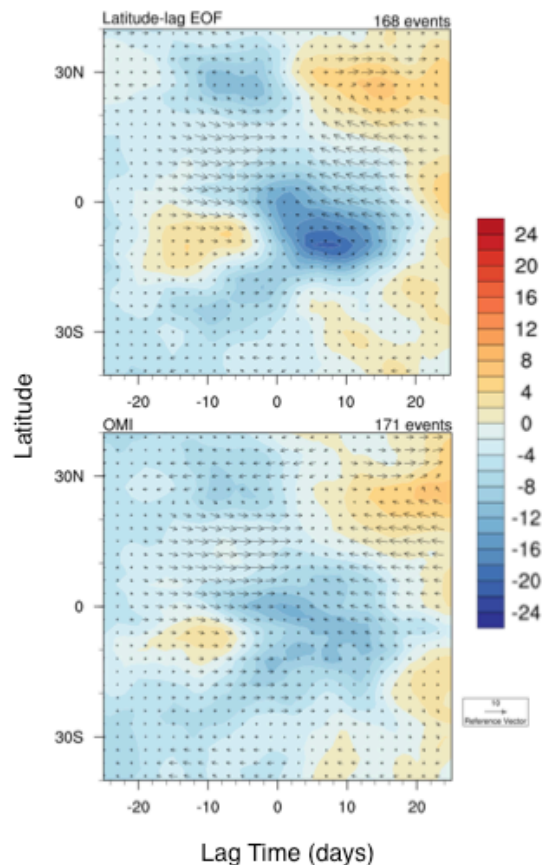


Figure 3: Latitude-lag diagram of the OLR anomaly and 200hPa winds averaged from 20-70E centered on phase 1 for IMMI and OMI.

displays a continuous eastward propagating MJO OLR signal of at least comparable strength to OMI. Latitude-lag diagrams of OLR anomalies and 200hPa winds for 20-70E (figure 3) show a more centered and distinct latitudinal and temporal structure in IMMI in comparison to OMI.

Figure 4 shows composite maps of the anomalous OLR with 200hPa winds at lags -5, 0, and 5. Over this time period, the winds over and to the north of the convective initiation region are becoming more easterly and southerly, providing outflow in both zonal and meridional directions.

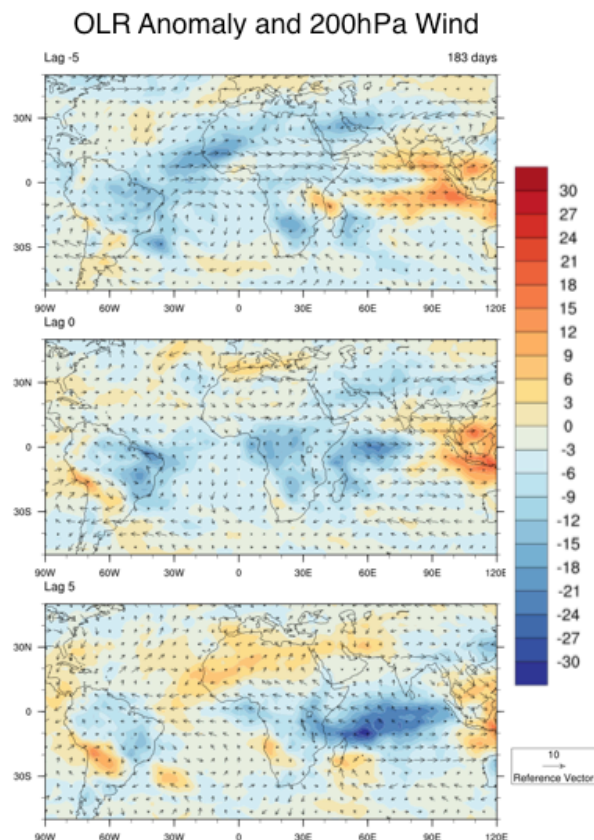


Figure 4: Composites of the OLR anomaly and 200hPa wind for lags of -5, 0, and +5 days from phase 1 for IMMI.

5. CONCLUSIONS

Composites created with the time-extended 20-70E latitudinal EOFs (IMMI) are able to capture a robust MJO signal, while emphasizing structure over eastern Africa, Southeast Asia, and the Indian Ocean. Furthermore, the presence of the extratropical signal in the leading two EOFs and the effectiveness of this index underline the frequency with which convection occurs with a distinct meridional progression over this region prior to MJO convective initiation. Since these precursors coincide with the arrival of upper-tropospheric divergence and meridional outflow over the

region, an upper-tropospheric momentum budget based on IMMI would be informative.

6. REFERENCES

- Barlow, M., M. Wheeler, B. Lyon, and H. Cullen, 2005: Modulation of daily precipitation over southwest Asia by the Madden Julian Oscillation. *Mon. Wea. Rev.*, **133**, 3579-3594.
- Dee, D. P., Uppala, S. M., Simmons, A. J., Berrisford, P., Poli, P., Kobayashi, S., Andrae, U., Balmaseda, M. A., Balsamo, G., Bauer, P., Bechtold, P., Beljaars, A. C. M., van de Berg, L., Bidlot, J., Bormann, N., Delsol, C., Dragani, R., Fuentes, M., Geer, A. J., Haimberger, L., Healy, S. B., Hersbach, H., Hólm, E. V., Isaksen, I., Kållberg, P., Köhler, M., Matricardi, M., McNally, A. P., Monge-Sanz, B. M., Morcrette, J.-J., Park, B.-K., Peubey, C., de Rosnay, P., Tavolato, C., Thépaut, J.-N. and Vitart, F., 2011: The ERA-Interim reanalysis: configuration and performance of the data assimilation system. *Q.J.R. Meteorol. Soc.*, **137**: 553–597. doi: 10.1002/qj.828
- Duchon C. E., 1979: Lanczos Filtering in One and Two Dimensions. *J. Appl. Meteor.*, **18**, 1016–1022. doi: [http://dx.doi.org/10.1175/1520-0450\(1979\)018<1016:LFIOAT>2.0.CO;2](http://dx.doi.org/10.1175/1520-0450(1979)018<1016:LFIOAT>2.0.CO;2)
- Kiladis G. N., J. Dias, K. H. Straub, M. C. Wheeler, S. N. Tulich, K. Kikuchi, K. M. Weickmann, and M. J. Ventrice, 2014: A Comparison of OLR and Circulation-Based Indices for Tracking the MJO. *Mon. Wea. Rev.*, **142**, 1697–1715. doi: <http://dx.doi.org/10.1175/MWR-D-13-00301.1>
- Liebmann, B., and C. A. Smith, 1996: Description of a complete (interpolated) outgoing longwave radiation dataset. *Bull. Amer. Meteor. Soc.* **77**, 1275-1277.
- Oettli, P., Tozuka, T., Izumo, T., Engelbrecht, F. A. and Yamagata, T., 2014: The self-organizing map, a new approach to apprehend the Madden–Julian Oscillation influence on the intraseasonal variability of rainfall in the southern African region. *Clim. Dyn.*, **43**, 1557–1573.
- Wheeler, M., and H. H. Hendon, 2004: An all-season real-time multivariate MJO index: Development of an index for monitoring and prediction. *Mon. Wea. Rev.*, **132**, 1917-1932.
- Zhang, C., 2005: The Madden-Julian Oscillation. *Rev. Geophys.*, **43**, RG2003, doi:10.1029/2004RG000158.